

RESEARCH NOTE

A comparative study of the molecular evolution of signalling pathway members across olfactory, gustatory and photosensory modalities

CHAO HE^{1,2}, DAVID A. FITZPATRICK³ and DAMIEN M. O'HALLORAN^{1,2*}

¹*Department of Biological Sciences, George Washington University, 333 Lisner Hall, 2023 G St. NW, Washington, DC 20052, USA*

²*Institute for Neuroscience, George Washington University, 636 Ross Hall, 2300 I St. NW, Washington DC 20037, USA*

³*Department of Biology, Genome Evolution Laboratory, National University of Ireland Maynooth, Maynooth, Co. Kildare, Ireland*

[He C., Fitzpatrick D. A. and O'halloran D. M. 2013 A comparative study of the molecular evolution of signalling pathway members across olfactory, gustatory and photosensory modalities. *J. Genet.* **92**, 327–334]

Introduction

All sensory modalities serve a similar objective, which is to decode input by making predictions in time and space about an animal's surroundings. The evolution of sensory modalities is driven by the need to shape effective behavioural outputs, and in turn increase survival. Throughout evolution, sensory systems have undergone a great deal of specialization; and even though some modalities are derived from unique origins within different phyla, they still exhibit many common design features (Strausfeld and Hildebrand 1999; Eisthen 2002; Jacobs *et al.* 2007). We now have detailed mechanistic data on how sensory systems operate within specific animals (Buck and Axel 1991; Chalasani *et al.* 2007; Sato *et al.* 2008; Wicher *et al.* 2008), however it is still not clear how sensory signalling pathways evolve at the molecular level, and whether these evolutionary mechanisms are shared between diverse taxa. Here we set out to investigate the molecular evolution of signalling pathway members across olfactory, gustatory, and photosensory modalities from very divergent phyla in an attempt to develop a model of molecular evolution for sensory systems. From our pairwise intraphylum analysis we found that sensory signalling pathways unusually undergo high levels of functional constraint that are higher than genomewide global levels of constraint, and this purifying selection is common within the very divergent taxa we examined. We also find that gene duplication events represent a conserved but heterogeneous driver of evolution within sensory signalling pathways. Taken together, we propose a 'sessile' mechanism of sensory signalling pathway evolution, which on one side

facilitates bursts of gene duplication and relaxed selection and on the other side it is unusually anchored by high levels of selective constraint that preserves core sensory function.

Materials and methods

Sequences

Sequences were sourced from the Kyoto Encyclopedia of Genes and Genomes (KEGG, <http://www.genome.jp/kegg/>) pathway database by following the data oriented entry point pathway. Pathways that were not represented at KEGG were sourced from Flybase ver. FB2012.05 (<http://flybase.org/>), and Wormbase ver. WS233 (<http://www.wormbase.org>). Only genes that had clear intraphylum orthologues from the database InParanoid7 (<http://inparanoid.sbc.su.se>) or OrthoDB (<http://cegg.unige.ch/orthodb6>) were selected and only reference (or longest) splice forms were included. Paralogues were sourced using maximum stringency settings from the KEGG pathway sequence similarity database (SSDB), which contains the information about amino acid sequence similarities among all protein-coding genes in completed genomes using Smith–Waterman similarity scoring and bidirectional best hits.

Phylogenetic analysis

Phylogenetic relationships were inferred by reconstructing phylogenies via maximum likelihood using PhyML (Guindon and Gascuel 2003). Orthologues were aligned using the multiple sequence alignment software MUSCLE ver. 3.8.31 (Edgar 2004), and gaps were systematically stripped from all sequences after alignment.

*For correspondence. E-mail: damienoh@gwu.edu.

Keywords. olfaction; gustation; photo-excitation; comparative evolution; divergence; molecular diversity; gene duplication.

Analysis of molecular data

Synonymous (d_S) and nonsynonymous (d_N) substitution rates for orthologues were estimated using the methods of Yang and Nielsen (2000) as implemented in yn00 in the PAML suite (Yang 1997; Yang and Nielsen 2000) using an intraphylum pairwise approach. To compare the frequency of substitutions at silent sites to that of nonsilent sites within each pathway to the frequency of substitutions at silent sites to that of nonsilent sites across the genomes of the taxa under examination, randomization testing was determined. Randomization analysis was performed by calculating the average d_N/d_S value for 50,000 randomly assembled groups of orthologous genes. Random networks were equal in size to the average size of our pathways and sampling permitted replacement. Only 1:1 protein coding orthologues that were represented by 100% bootstrap support at InParanoid7 were included. Measures of nucleotide diversity (π) were performed using DnaSP ver. 5 (Librado and Rozas 2009) from multiple sequence alignments generated using the software MUSCLE ver. 3.8.31 (Edgar 2004). The average paranome size within each phylum was computed by firstly performing a blast-all-against-all search within each genome and then generating groups using the Markov clustering algorithm (MCL), <http://micans.org/mcl/index.html>.

Statistics

All averaged data are expressed as mean \pm SEM. Statistical analysis was performed with Student's t -test and $P < 0.05$ was considered statistically significant. Gene duplication correlations were measured using the nonparametric Spearman's rank correlation coefficient (r_s) test, and also using the Pearson product-moment correlation coefficient (r) using R project: <http://www.r-project.org/>.

Results

To examine the rate of divergence across olfactory, gustatory, and photosensory modalities within each of three phyla (Nematoda, Arthropoda and Chordata), we downloaded signalling pathway genes from KEGG. Pathways that were not represented at KEGG were sourced from flybase and wormbase databases. From this we compiled a list of genes in each sensory modality from the nematodes *Caenorhabditis elegans* and *C. briggsae*; from the insects *Drosophila melanogaster* and *Anopheles gambiae*; and from the mammalian species, human and mouse. Next we screened for those genes that are clear intraphylum orthologues between *C. elegans* and *C. briggsae*, or between *D. melanogaster* and *A. gambiae*, or between human and mouse (table 1). We examined the divergence rate between each pairing by comparing substitutions at silent sites to that of nonsilent sites for each intraphylum orthologous pairing. By comparing the average rate of divergence for all paralogues from each sensory modality we found that in each modality the

divergence rate was not significantly different (figure 1, A–B; $P = 0.6$ for olfaction d_N/d_S versus gustation; $P = 0.5$ for olfaction d_N/d_S versus phototransduction d_N/d_S ; $P = 0.62$ for gustation d_N/d_S versus phototransduction d_N/d_S ; $P = 0.07$ for olfaction d_N versus gustation d_N ; $P = 0.3$ for olfaction d_N versus phototransduction d_N ; $P = 0.28$ for gustation d_N versus phototransduction d_N). We also determined the average extent of molecular diversity (π) for each orthologue pairing, and found that in case of diversity there was no significant difference between modalities (figure 1C; $P = 0.1$ for olfaction versus gustation; $P = 0.3$ for olfaction versus phototransduction; $P = 0.7$ for gustation versus phototransduction).

Overall, we found that each modality is undergoing purifying selection (figure 1A). To place this rate of selection in a context of global divergence within each phylum we examined genomewide rates of divergence for: *C. elegans* versus *C. briggsae*; *D. melanogaster* versus *A. gambiae*; and for human versus mouse. We then generated randomized data sets (50,000 in total) within each phylum and examined the frequency of mean d_N/d_S values in each case (figure 1, D–F). From this analysis we found an average d_N/d_S value = 0.14 for human versus mouse, which is over 1.5 times higher than the average d_N/d_S level within the olfactory signalling pathway (blue arrow), and over 2.5 times higher than the average d_N/d_S level within the gustatory pathway (red arrow), or phototransduction pathway (green arrow) in mammals. In case of *Drosophila* versus *Anopheles*, we found an average d_N/d_S across the genome of 0.11; this value is over five times higher than the average d_N/d_S value for the olfactory signalling pathway (blue arrow), and almost an order of magnitude higher ($9.5\times$) than the average for the gustatory signalling pathway (red arrow), and almost 20 times higher (18.4) than the average value for the phototransduction cascade (green arrow) between flies and mosquitoes. In case of *Caenorhabditis*, we found an average d_N/d_S value of 0.08, which is between two to three times higher than the average constraint that is observed for the olfactory (blue arrow), gustatory (red arrow), or phototransduction (green arrow) cascades between *C. elegans* and *C. briggsae*. Our randomization data are consistent with previous reports on global d_N/d_S range (Stein et al. 2003; Wang et al. 2007), and taken together with our data on sensory signalling pathways, this suggests that the overall conserved sensory signalling cascade members are under more functional constraint than the average level of global constraint across the genome in each case. Interestingly, we observed most constraint for the phylum Arthropoda, with the highest level of constraint detected for the phototransduction cascade, followed next by taste signalling, and then olfaction.

Next we examined the extent of gene duplication for each modality within each phylum by comparing the number of paralogues for each member of each signalling pathway. From this analysis we found significant gene duplications in each phylum and for each modality. Moreover, we revealed that in each phylum the extent of gene duplication was

Table 1. List of genes, accession numbers, and the encoded proteins of all loci examined.

Gene	⁷ KEGG id	Ortholog	KEGG id	Protein
Phylum chordata				
¹ <i>H. sap</i> Arrestin	409	² <i>M. mus</i> Arrestin	216869	Beta arrestin-2
<i>H. sap</i> PKA	5613	<i>M. mus</i> PKA	19108	Protein kinase A
<i>H. sap</i> PKG	5593	<i>M. mus</i> PKG	19092	Protein kinase G
<i>H. sap</i> GCAP	2978	<i>M. mus</i> GCAP	14913	Guanylate cyclase activator 1C
<i>H. sap</i> G-olf	2774	<i>M. mus</i> G-olf	14680	G protein G(olf) subunit alpha
<i>H. sap</i> CaMKII	817	<i>M. mus</i> CaMKII	108058	Ca ²⁺ /CaM-dependent protein kinase II δ
<i>H. sap</i> CaM	801	<i>M. mus</i> CaM	12313	Calmodulin
<i>H. sap</i> CNG	54714	<i>M. mus</i> CNG	30952	Cyclic nucleotide gated channel beta 3
<i>H. sap</i> AC	109	<i>M. mus</i> AC	104111	Adenylate cyclase
<i>H. sap</i> R	81466	<i>M. mus</i> R	258937	Olfactory receptor
<i>H. sap</i> R1	10798	<i>M. mus</i> R1	258640	Olfactory receptor
<i>H. sap</i> R2	119687	<i>M. mus</i> R2	258248	Olfactory receptor
<i>H. sap</i> CLC α	1179	<i>M. mus</i> CLC α	23844	Chloride channel calcium activated
<i>H. sap</i> Phosducin	5132	<i>M. mus</i> Phosducin	20028	Phosducin
<i>H. sap</i> Gustducin	346562	<i>M. mus</i> Gustducin	242851	G-protein G(t) subunit alpha
<i>H. sap</i> GNB1	2782	<i>M. mus</i> GNB1	14688	G protein beta subunit
<i>H. sap</i> T1R	83756	<i>M. mus</i> T1R	83771	Taste receptor
<i>H. sap</i> PDE	5136	<i>M. mus</i> PDE	18573	Calmodulin-dependent phosphodiesterase
<i>H. sap</i> PLC β	5330	<i>M. mus</i> PLC β	18796	Phospholipase C beta
<i>H. sap</i> CaCN	773	<i>M. mus</i> CaCN	12286	Voltage-dependent calcium channel P/Q type
<i>H. sap</i> KCN	3745	<i>M. mus</i> KCN	16500	Potassium voltage-gated channel
<i>H. sap</i> PKA	5566	<i>M. mus</i> PKA	18747	Protein kinase A (olfactory)
<i>H. sap</i> AC	196883	<i>M. mus</i> AC	104110	Adenylate cyclase
<i>H. sap</i> ENaC	6337	<i>M. mus</i> ENaC	20276	Non voltage-gated sodium channel 1 alpha
<i>H. sap</i> Rec	5957	<i>M. mus</i> Rec	19674	Recoverin
<i>H. sap</i> Rh	6010	<i>M. mus</i> Rh	212541	Rhodopsin
<i>H. sap</i> Arr	408	<i>M. mus</i> Arr	109689	Beta arrestin-1
<i>H. sap</i> Gt	2779	<i>M. mus</i> Gt	14685	G-protein subunit alpha
<i>H. sap</i> RGS9	8787	<i>M. mus</i> RGS9	19739	Regulator of G protein signaling
<i>H. sap</i> PDE	5145	<i>M. mus</i> PDE	225600	cGMP phosphodiesterase
<i>H. sap</i> GC	2986	<i>M. mus</i> GC	245650	Guanylate cyclase 2f
<i>H. sap</i> NCKX	9187	<i>M. mus</i> NCKX	214111	Sodium/potassium/calcium exchanger
<i>H. sap</i> CNG	1259	<i>M. mus</i> CNG	12788	Cyclic nucleotide gated channel alpha 1
Phylum arthropoda				
³ <i>D. me</i> Ir8a-PA	Dmel_CG32704	⁴ <i>A. ga</i> Ir8a	AgaP_AGAP010411	Ionotropic glutamate receptor
<i>D. me</i> Galpha	Dmel_CG17759	<i>A. ga</i> Galpha	AgaP_AGAP005079	G protein alpha subunit
<i>D. me</i> eag	Dmel_CG10952	<i>A. ga</i> eag	AgaP_AGAP002719	Voltage gated cation channel
<i>D. me</i> geko	Dmel_CG13695	<i>A. ga</i> geko	AgaP_AGAP005168	Novel olfactory Gene
<i>D. me</i> orco	Dmel_CG10609	<i>A. ga</i> orco	AgaP_AGAP002560	Odorant receptor co-receptor
<i>D. me</i> dunce	Dmel_CG32498	<i>A. ga</i> dunce	AgaP_AGAP000236	cAMP phosphodiesterase
<i>D. me</i> gcy 89da	Dmel_CG14885	<i>A. ga</i> gcy 89da	AgaP_AGAP004564	Atypical soluble guanylyl cyclase
<i>D. me</i> gr5a	Dmel_CG15779	<i>A. ga</i> gr5a	AgaP_AGAP003253	Sweet taste receptor
<i>D. me</i> gr66a	Dmel_CG7189	<i>A. ga</i> gr66a	AgaP_AGAP002275	Gustatory receptor
<i>D. me</i> goa 47a	Dmel_CG2204	<i>A. ga</i> goa 47a	AgaP_AGAP005773	G protein alpha subunit
<i>D. me</i> TRPA1	Dmel_CG5751	<i>A. ga</i> TRPA1	AgaP_AGAP004863	Transient receptor potential (TRP) A1
<i>D. me</i> AC78c	Dmel_CG10564	<i>A. ga</i> AC78c	AgaP_AGAP002262	Adenylyl cyclase
<i>D. me</i> Gq	Dmel_CG17759	<i>A. ga</i> Gq	AgaP_AGAP005079	G protein alpha subunit
<i>D. me</i> PLC β	Dmel_CG3620	<i>A. ga</i> PLC β	AgaP_AGAP001936	Phosphatidylinositol phospholipase C
<i>D. me</i> PKC	Dmel_CG6518	<i>A. ga</i> PKC	AgaP_AGAP012252	Protein kinase C
<i>D. me</i> TRP	Dmel_CG5996	<i>A. ga</i> TRP	AgaP_AGAP008435	TRP cation channel family C
<i>D. me</i> TRPL	Dmel_CG18345	<i>A. ga</i> TRPL	AgaP_AGAP010630	TRP-like cation channel
<i>D. me</i> CaM	Dmel_CG8472	<i>A. ga</i> CaM	AgaP_AGAP010957	Calmodulin
<i>D. me</i> Arr-2	Dmel_CG5962	<i>A. ga</i> Arr-2	AgaP_AGAP006263	Phototransduction arrestin
<i>D. me</i> INAD	Dmel_CG3504	<i>A. ga</i> INAD	AgaP_AGAP002145	Inactivation-no-after-potential D protein
<i>D. me</i> NINAC	Dmel_CG5125	<i>A. ga</i> NINAC	AgaP_AGAP009730	Neither inactivation nor after potential C
<i>D. me</i> IP3R	Dmel_CG1063	<i>A. ga</i> IP3R	AgaP_AGAP006475	Inositol 1,4,5-triphosphate receptor

Table 1. (contd.)

Gene	⁷ KEGG id	Ortholog	KEGG id	Protein
Phylum nematoda				
⁵ <i>C. el</i> odr-10	CELE_C53B7.5	⁶ <i>C. br</i> odr-10	CBG10912	De-orphaned olfactory receptor
<i>C. el</i> str-2	CELE_C50C10.7	<i>C. br</i> str-2	CBG19383	Orphan olfactory receptor
<i>C. el</i> str-1	CELE_C42D4.5	<i>C. br</i> str-1	CBG05794	Orphan olfactory receptor
<i>C. el</i> arr-1	CELE_F53H8.2	<i>C. br</i> arr-1	CBG08085	Arrestin
<i>C. el</i> rgs-3	CELE_C29H12.3	<i>C. br</i> rgs-3	CBG02574	Regulator of G protein signaling
<i>C. el</i> grk-2	CELE_W02B3.2	<i>C. br</i> grk-2	CBG15249	G-protein receptor kinase
<i>C. el</i> odr-3	CELE_C34D1.3	<i>C. br</i> odr-3	CBG09409	G protein alpha subunit
<i>C. el</i> egl-4	CELE_F55A8.2	<i>C. br</i> egl-4	CBG08401	Protein kinase G
<i>C. el</i> tax-2	CELE_F36F2.5	<i>C. br</i> tax-2	CBG12422	CNG channel beta subunit
<i>C. el</i> tax-4	CELE_ZC84.2	<i>C. br</i> tax-4	CBG06949	CNG channel alpha subunit
<i>C. el</i> odr-1	CELE_R01E6.1	<i>C. br</i> odr-1	CBG07425	Receptor guanylyl cyclase
<i>C. el</i> daf-11	CELE_B0240.3	<i>C. br</i> daf-11	CBG23280	Receptor guanylyl cyclase
<i>C. el</i> gpa-3	CELE_E02C12.5	<i>C. br</i> gpa-3	CBG19263	G protein alpha subunit
<i>C. el</i> gpc-1	CELE_K02A4.2	<i>C. br</i> gpc-1	CBG00049	G protein gamma subunit
<i>C. el</i> gcy-7	CELE_F52E1.4	<i>C. br</i> gcy-7	CBG11271	Receptor guanylyl cyclase
<i>C. el</i> gcy-5	CELE_ZK970.6	<i>C. br</i> gcy-5	CBG00850	Receptor guanylyl cyclase
<i>C. el</i> osm-9	CELE_B0212.5	<i>C. br</i> osm-9	CBG15022	TRP cation channel
<i>C. el</i> lite-1	CELE_C14F11.3	<i>C. br</i> lite-1	CBG05007	Light activated 8-TM protein
<i>C. el</i> goa-1	CELE_C26C6.2	<i>C. br</i> goa-1	CBG24698	G protein alpha subunit
<i>C. el</i> pde-1	CELE_T04D3.3	<i>C. br</i> pde-1	CBG20362	cGMP phosphodiesterase
<i>C. el</i> pde-2	CELE_R08D7.6	<i>C. br</i> pde-2	CBG06847	cGMP phosphodiesterase
<i>C. el</i> pde-5	CELE_C32E12.2	<i>C. br</i> pde-5	CBG12836	cGMP phosphodiesterase

¹*H. sap* refers to *Homo sapiens*

²*M. mus* refers to *Mus musculus*

³*D. me* refers to *Drosophila melanogaster*

⁴*A. ga* refers to *Anopheles gambiae*

⁵*C. el* refers to *Caenorhabditis elegans*

⁶*C. br* refers to *Caenorhabditis briggsae*

⁷KEGG refers to the 'Kyoto Encyclopedia of Genes and Genomes' (<http://www.genome.jp/kegg/>).

highest for the olfactory modality, and this was especially true for nematodes and mammals where the number of duplicates were significantly higher for the olfactory signalling pathway when compared with the phototransduction cascade (figure 2A, $P = 0.02$ for *C. elegans* olfactory versus *C. elegans* phototransduction; $P = 0.023$ for *C. briggsae* olfactory versus *C. briggsae* phototransduction; $P = 0.02$ for mouse olfactory versus mouse phototransduction; $P = 0.03$ for human olfactory versus human phototransduction). By averaging the number of paralogues across all phyla and partitioning by sensory modality we observe almost seven times as many duplicates within the olfactory circuit than the phototransduction circuit, and over four times as many paralogues for the olfactory circuit than the gustatory circuit (figure 2B), revealing a modality specific expansion of the olfactory circuit. To develop an understanding of global levels of gene duplication within each phylum, we generated the paranome (number of proteins with one or more paralogues) for *C. elegans*, *D. melanogaster*, and *Mus musculus* using the MCL clustering algorithm (<http://micans.org/mcl/>) and found the median gene family to be between two and three members in size. The difference in global gene family size compared with gene families within sensory systems (figure 2B) clearly underscores the extent to which gene

duplication impacts the sensory systems and highlights the striking spike in gene duplication observed within the olfactory system, and to a lesser extent the gustatory and photosensory systems (figure 2B). Following this we examined the level of concordance for gene duplication events for each phylum and within each sensory modality. For each sensory modality we observed robust correlations between the number of paralogues within each modality (figure 2, C–E: i, nematode; ii, insect; iii, mammal—significance at $P < 0.001$ using Spearman rank-order correlation coefficient, r_s , and coefficient of determination, r^2). Within arthropods overall we observed more narrow expansions (figure 2A). We also observed fewer clear orthologues within the sensory systems of *D. melanogaster* and *A. gambiae* (figure 2, Cii–Eii), likely reflecting in part their more ancient divergence estimate of 250 mya (Gaunt and Miles 2002). As mentioned above, we also observed most constraint within the arthropod sensory pathway, which also likely reflects this greater evolutionary distance as we only included orthologues supported by 100% bootstrap support. Divergence estimates for human with mouse and *C. elegans* with *C. briggsae* are between 80–95 mya (Nei et al. 2001; Stein et al. 2003). We also observed a significantly reduced olfactory receptor repertoire in humans when compared to mouse (figure 2 Ciii) which is

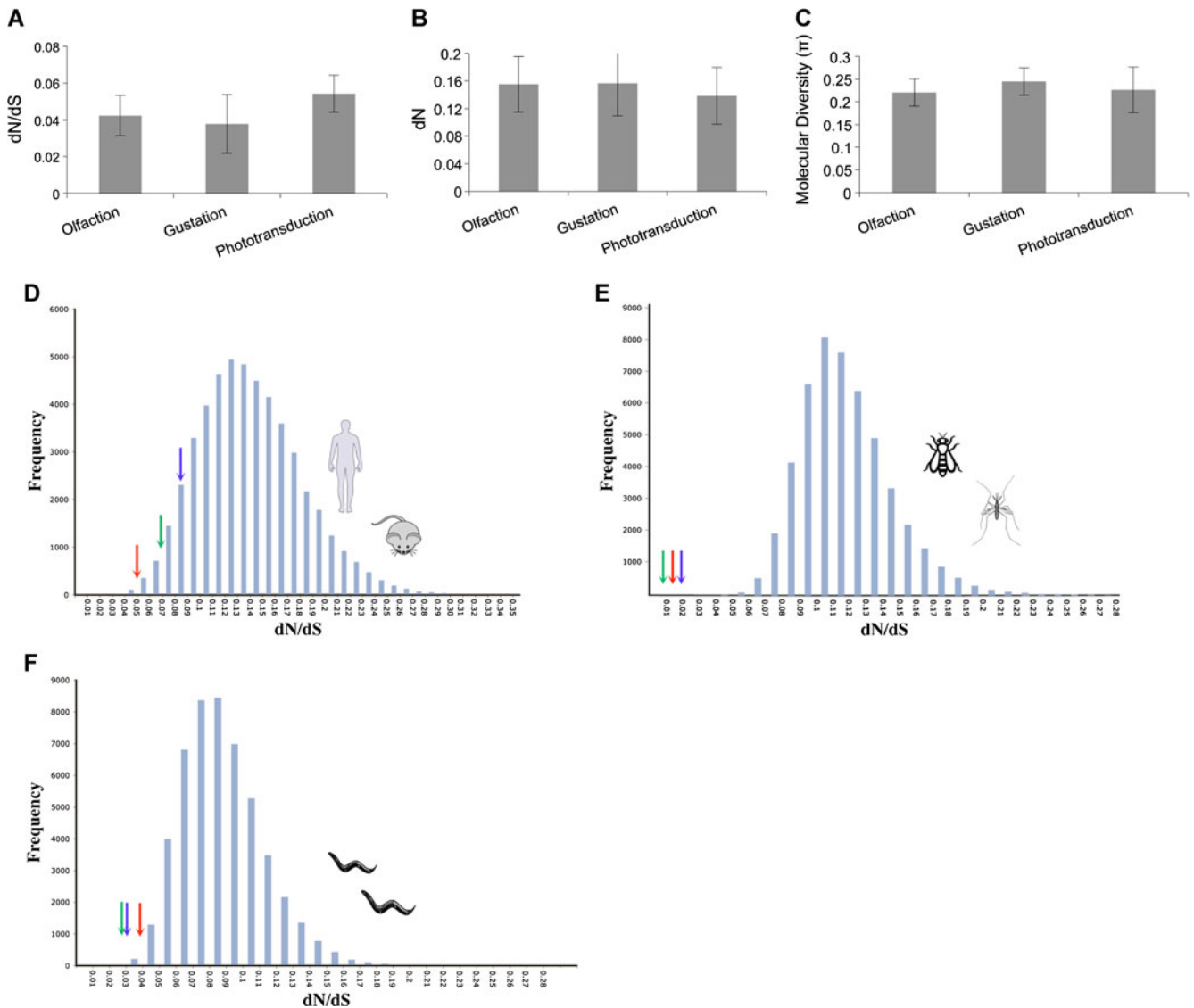


Figure 1. Average rates of divergence and diversity across all phyla partitioned by sensory modality. (A) Plot of average divergence values for each sensory modality from nematodes, insects and mammals. (B) Plot of average number of nonsynonymous substitutions per nonsynonymous site for each sensory system from nematodes, insects and mammals. (C) Plot of average molecular diversity for each sensory system across nematodes, insects, and mammals. Error bars represent the standard error of the mean. (D–F) Frequency distribution of average d_N/d_S values from 50,000 randomization sets (blue bars) comprising orthologous groupings from mammals (D), insects (E) and nematodes (F). The x -axis in each case represents binned divergence categories plotted against the frequency on the y -axis. The blue arrows indicate the average d_N/d_S value of the olfactory sensory system in each case, the red arrows indicates the average d_N/d_S value of the gustatory network in each case, and the green arrows indicates the average d_N/d_S value of the photoexcitation cascade in each case.

consistent with previous descriptions of the human olfactory receptor family (Young *et al.* 2002).

Discussion

Purifying selection and sensory systems

From our results we found that the overall function of conserved signalling pathway members within the olfactory, gustatory, and photoexcitation systems is preserved through intense constraint at the molecular level which is higher than the level of global constraint across the genome in each case.

By examining gene duplication events within each sensory system, we observed significant expansions in each case, with the olfactory system exhibiting the greatest number of duplicates. Taken together our data suggests that sensory systems appear to evolve largely through gene duplication events, which provides a pool of new genes that likely undergo such a relaxed level of selective constraint that identifying clear orthologues is very difficult and not likely to be detected through our analysis. However, in order to balance this strategy of large gene duplication events, the core signalling pathway members endure unusually strong purifying selection to preserve their critical function.

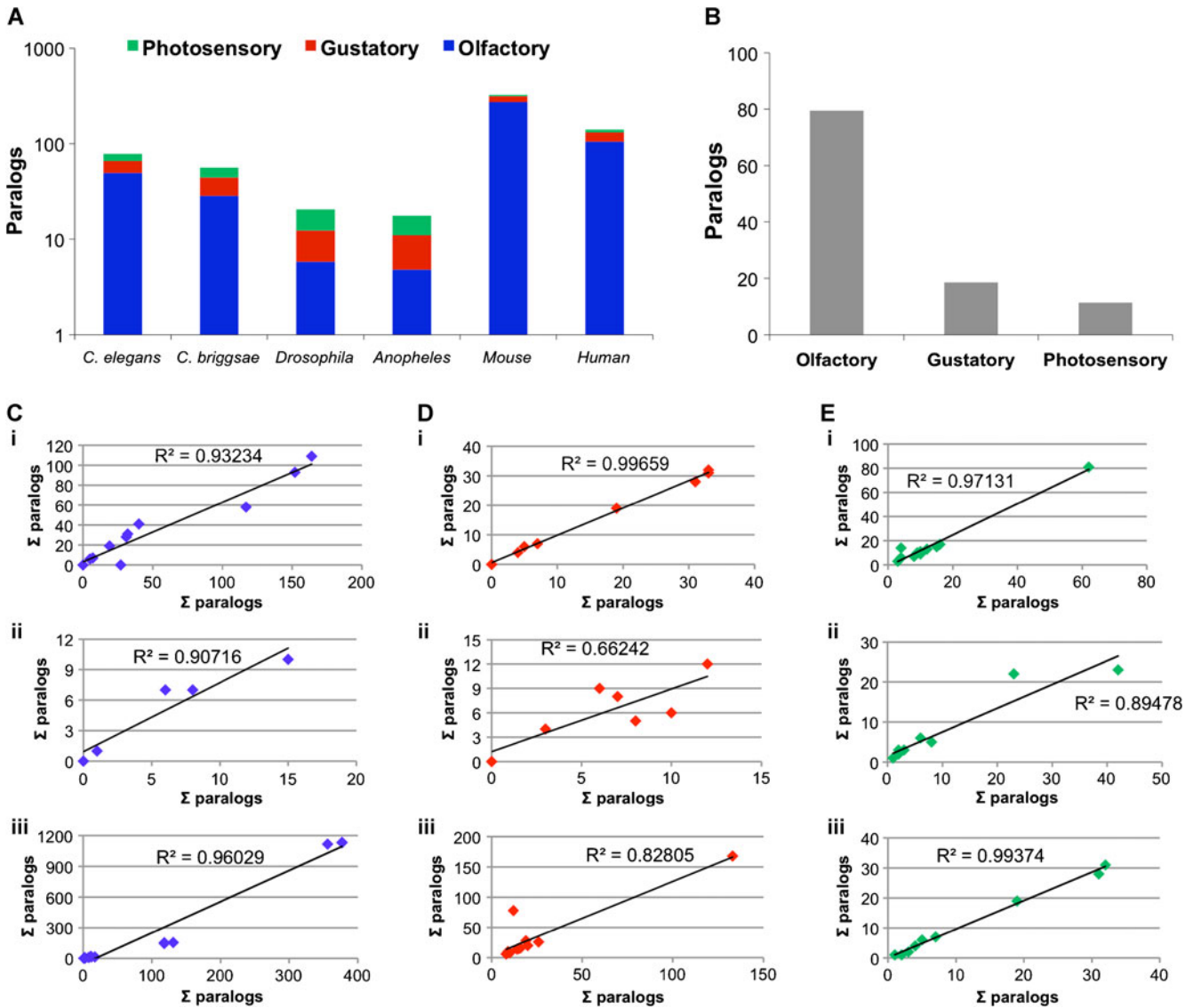


Figure 2. Gene duplication forms a source of novelty for all sensory modalities, in particular the olfactory circuit. (A) Box plots representing the total paralogue count (log scale) for each signalling pathway partitioned by sensory modality and species. (B) Average number of paralogs for each sensory modality across all phyla organized by sensory modality. (C–E) Graphs plotting correlation of the concordance between the number of paralogs within each phylum (i, nematode; ii, insect; iii, mammal) for the olfactory (C, i–iii), gustatory (D, i–iii), and photoexcitation (E, i–iii) pathways.

Gene duplication and sensory systems: a heterogeneous strategy?

The olfactory system is charged with decoding an incredibly diverse array of distinct stimuli. Olfactory receptor neurons converge onto the olfactory bulb in mammals, and the antennal lobe in *Drosophila* (Buck 2000; Hallem et al. 2006; Vosshall and Stocker 2007). In each case, multiple olfactory neurons project onto overlapping glomeruli, which help decrease noise and heightens sensitivity. In *C. elegans* there are multiple olfactory receptors expressed per primary sensory neuron (Troemel et al. 1995). Within the olfactory system, new receptors can generate entirely new sensory input, and new regulators can create novelty by modulat-

ing tuning, increasing discriminatory power or accelerating processing speed. Therefore, in the olfactory systems of nematodes, insects and mammals, gene duplication events may serve as the ideal mode of flexibility to maximize predictions about the environment while only incrementally modulating energy demands. Unlike the olfactory system, gene duplications of signalling machinery, and thus architecture, of the visual system in mammals and insects would likely require great energy demands but perhaps only achieve more resolving power. In *C. elegans* the photosensory circuit facilitates a basic nonocular phototaxis response that references an animal’s orientation within the soil by detecting short wavelength light, and so genetic accretion may have

a limited benefit within the photosensory circuit of *C. elegans* (Edwards *et al.* 2008; Liu *et al.* 2010). The gustatory system may represent a hybrid state as the benefits of gene duplication may be similar to those in the olfactory system in that new gustatory input could be generated through novelty. However, unlike the olfactory system, the gustatory architecture is more complex in insects and mammals, and so the energy costs associated with more novelty may outweigh the benefits. In *Drosophila*, the gustatory organs are distributed over the entire body (Voshall and Stocker 2007). Unlike the antennal lobe of the olfactory system of *Drosophila*, the gustatory neurons all over the body target the suboesophageal ganglion (SOG), and unlike the antennal lobe, the SOG does not exhibit any structural divisions such as the glomeruli of the olfactory system (Voshall and Stocker 2007). Further, in mammals the gustatory receptors are partitioned into specialized cells that decode specific tastes (sweet, sour, salty, bitter and umami), and each receptor employs a different form of signal transduction (Chandrashekar *et al.* 2006; Huang *et al.* 2006). Therefore, the benefits of genetic accretion at the receptor or even regulator level may only benefit a specific subclass of gustatory receptor neurons, and this compartmentalization perhaps dilutes, relatively at least, the selective pressure driving novelty through gene expansion across the gustatory circuit.

Conclusion

The goal of our analysis was to conduct a pair wise examination of the molecular evolution of sensory signalling pathways within divergent phyla. From this analysis we have found that sensory signalling pathway members undergo unusually high levels of constraint which are in fact higher than the level of global constraint across the genome in each case. However, within each signalling pathway we also reveal a conserved theme of large gene duplication events which are conserved within each phylum. These findings lead us to suggest a 'sessile' mechanism of sensory pathway evolution, which on one side facilitates bursts of gene duplications and relaxed selection, and on the other side is anchored by unusually high levels of selective constraint that preserve core sensory functions. Our findings are not a complete picture of how sensory modalities can evolve, but it is our hope that as more molecular data emerges on sensory circuits within diverse systems, it will yield more detailed models and descriptions of the molecular evolution of sensory signalling pathways, and through this analysis we can ultimately build a robust *evo-devo* picture of how sensory systems evolve.

Acknowledgements

We would like to thank The George Washington University Columbian College of Arts and Sciences and Department of Biological Sciences for funding to D. O'Halloran and C. He. We thank our anonymous reviewers for their helpful feedback and suggestions.

References

- Buck L. B. 2000 The molecular architecture of odor and pheromone sensing in mammals. *Cell* **100**, 611–618.
- Buck L. and Axel R. 1991 A novel multigene family may encode olfactory receptors: a molecular basis for odor recognition. *Cell* **65**, 175–187.
- Chalasan S. H., Chronis N., Tsunozaki M., Gray J. M., Ramot D., Goodman M. B. and Bargmann C. I. 2007 Dissecting a circuit for olfactory behaviour in *Caenorhabditis elegans*. *Nature* **450**, 63–70.
- Chandrashekar J., Hoon M. A., Ryba N. J. and Zuker C. S. 2006 The receptors and cells for mammalian taste. *Nature* **444**, 288–294.
- Edgar R. C. 2004 MUSCLE: a multiple sequence alignment method with reduced time and space complexity. *BMC Bioinformatics* **5**, 113.
- Edwards S. L., Charlie N. K., Milfort M. C., Brown B. S., Gravelin C. N., Knecht J. E. and Miller K. G. 2008 A novel molecular solution for ultraviolet light detection in *Caenorhabditis elegans*. *PLoS Biol.* **6**, e198.
- Eisthen H. L. 2002 Why are olfactory systems of different animals so similar? *Brain Behav. Evol.* **59**, 273–293.
- Gaunt M. W. and Miles M. A. 2002 An insect molecular clock dates the origin of the insects and accords with palaeontological and biogeographic landmarks. *Mol. Biol. Evol.* **19**, 748–761.
- Guindon S. and Gascuel O. 2003 A simple, fast, and accurate algorithm to estimate large phylogenies by maximum likelihood. *Syst. Biol.* **52**, 696–704.
- Hallen E. A., Dahanukar A. and Carlson J. R. 2006 Insect odor and taste receptors. *Annu. Rev. Entomol.* **51**, 113–135.
- Huang A. L., Chen X., Hoon M. A., Chandrashekar J., Guo W., Tränkner D. *et al.* 2006 The cells and logic for mammalian sour taste detection. *Nature* **442**, 934–938.
- Jacobs D. K., Nakanishi N., Yuan D., Camara A., Nichols S. A. and Hartenstein V. 2007 Evolution of sensory structures in basal metazoa. *Integr. Comp. Biol.* **47**, 712–723.
- Librado P. and Rozas J. 2009 DnaSP v5: a software for comprehensive analysis of DNA polymorphism data. *Bioinformatics* **25**, 1451–1452.
- Liu J., Ward A., Gao J., Dong Y., Nishio N., Inada H. *et al.* 2010 *C. elegans* phototransduction requires a G protein-dependent cGMP pathway and a taste receptor homolog. *Nat. Neurosci.* **13**, 715–722.
- Nei M., Xu P. and Glazko G. 2001 Estimation of divergence times from multiprotein sequences for a few mammalian species and several distantly related organisms. *Proc. Natl. Acad. Sci. USA* **98**, 2497–2502.
- Sato K., Pellegrino M., Nakagawa, T., Nakagawa, T., Voshall, L. B. and Touhara K. 2008 Insect olfactory receptors are heteromeric ligand-gated ion channels. *Nature* **452**, 1002–1006.
- Strausfeld N. J. and Hildebrand J. G. 1999 Olfactory systems: common design, uncommon origins? *Curr. Opin. Neurobiol.* **9**, 634–639.
- Stein L. D., Bao Z., Blasiar D., Blumenthal T., Brent M. R., Chen N. *et al.* 2003 The genome sequence of *Caenorhabditis briggsae*: a platform for comparative genomics. *PLoS Biol.* **2**, e45.
- Troemel E. R., Chou J. H., Dwyer N. D., Colbert H. A. and Bargmann C. I. 1995 Divergent seven transmembrane receptors are candidate chemosensory receptors in *C. elegans*. *Cell* **83**, 207–218.
- Voshall L. B. and Stocker R. F. 2007 Molecular architecture of smell and taste in *Drosophila*. *Annu. Rev. Neurosci.* **30**, 505–533.
- Wang H. Y., Chien H. C., Osada N., Hashimoto K., Sugano S., Gojobori T. *et al.* 2007 Rate of evolution in brain-expressed genes in humans and other primates. *PLoS Biol.* **5**, e13.

- Wicher D., Schäfer R., Bauernfeind R., Stensmyr M. C., Heller R., Heinemann S. H. and Hansson B. S. 2008 *Drosophila* odorant receptors are both ligand-gated and cyclic-nucleotide-activated cation channels. *Nature* **452**, 1007–1011.
- Yang Z. 1997 PAML: a program package for the phylogenetic analysis by maximum likelihood. Computer applications in the biosciences. *Cabios* **13**, 555–556.
- Yang Z. and Nielsen R. 2000 Estimating synonymous and nonsynonymous substitution rates under realistic evolutionary models. *Mol. Biol. Evol.* **17**, 32–43.
- Young J. M., Friedman C., Williams E. M., Ross J. A., Tonnes-Priddy L. and Trask B. J. 2002 Different evolutionary processes shaped the mouse and human olfactory receptor gene families. *Hum. Mol. Genet.* **11**, 535–546.

Received 12 February 2013, in final revised form 30 April 2013; accepted 2 May 2013
Published on the Web: 5 August 2013